

Molecular-Mechanical Switch-Based Solid-State Electrochromic Devices\*\*

David W. Steuerman, Hsian-Rong Tseng, Andrea J. Peters, Amar H. Flood, Jan O. Jeppesen, Kent A. Nielsen, J. Fraser Stoddart,\* and James R. Heath\*

The dynamics of electrochemically driven, bistable molecular mechanical switches—such as certain nondegenerate, two-station, donor–acceptor [2]catenanes and [2]rotaxanes—have been the subject of numerous experimental investigations<sup>[1–3]</sup> in the solution phase, in which the general mechanistic details of the redox-activated switching processes are becoming increasingly well understood.<sup>[4]</sup> These molecular machines may have many technological applications,<sup>[5]</sup> although few are likely to be liquid-solution-phase based.<sup>[6–9]</sup> Thus, significant effort has been directed towards understanding and exploiting the bistability of [2]catenanes and [2]rotaxanes in other environments, including both Langmuir–Blodgett (LB)<sup>[10,11]</sup> and self-assembled monolayers (SAMs),<sup>[12]</sup> and in solid-state molecular-switch tunnel junctions (MSTJs).<sup>[13–16]</sup>

Herein we explore, at a fundamental level, the solid-state application of electrochromic devices by taking advantage of the colorimetric changes that accompany the electrochemically driven switching of certain bistable [2]catenanes and [2]rotaxanes. The molecular switches were immobilized within a solid-state polymer electrolyte, and a microfabricated, planar, three-terminal equivalent of a standard electrochemical cell was used for electrical addressing. The polymer environment significantly slows down certain steps within the molecular-mechanical switching cycle, but the overall mechanism remains unchanged from that observed in other environments. We also find that by varying the molecular structure of the switch, the colorimetric retentions times of

these devices could be controlled over a dynamic range of 10<sup>3</sup> to 10<sup>4</sup> s. The fundamental properties of these devices were quantified through time- and temperature-dependent cyclic voltammetry (CV) measurements. In this way, the kinetic parameters ( $\Delta G^\ddagger$ ,  $\Delta H^\ddagger$ ,  $\Delta S^\ddagger$ , and  $E_a$ ) of the rate-limiting step in the switching cycle of the device could be evaluated for several different molecular switches.

Four bistable molecular-mechanical systems<sup>[2,3a,17,18]</sup>—two [2]catenanes **C1<sup>4+</sup>** and **C2<sup>4+</sup>** and two [2]rotaxanes **R1<sup>4+</sup>** and **R2<sup>4+</sup>**—along with appropriate control compounds, were investigated (Figure 1) for electrochromic device applica-

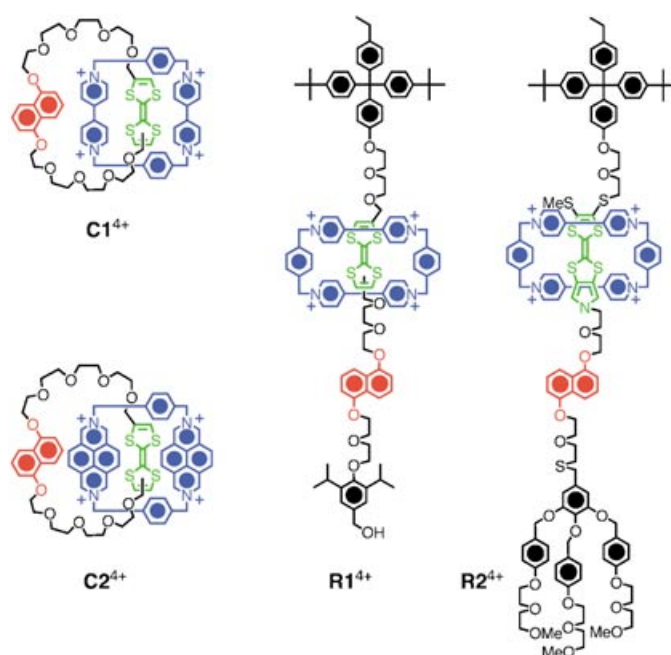


Figure 1. The structural formulas of the two bistable [2]catenanes **C1<sup>4+</sup>** and **C2<sup>4+</sup>** and the two bistable [2]rotaxanes **R1<sup>4+</sup>** and **R2<sup>4+</sup>** investigated within solid-state polymer electrolyte environments. The use of color—namely, red, blue, and green—for certain units and components relates to the graphical representations shown in Figure 2.

[\*] Dr. D. W. Steuerman, Dr. H.-R. Tseng, Dr. A. J. Peters, Dr. A. H. Flood, Dr. J. O. Jeppesen, K. A. Nielsen, Prof. J. F. Stoddart  
The California NanoSystems Institute, and  
Department of Chemistry and Biochemistry  
University of California, Los Angeles  
405 Hilgard Avenue, Los Angeles, CA 90095-1569 (USA)  
Fax: (+1) 310-206-1843  
E-mail: stoddart@chem.ucla.edu

Prof. J. R. Heath  
Division of Chemistry and Chemical Engineering, MC 127-72  
California Institute of Technology  
1200 East California Boulevard, Pasadena, CA 91125 (USA)  
Fax: (+1) 626-395-2355  
E-mail: heath@caltech.edu

[\*\*] This research was funded by the Office of Naval Research, the National Science Foundation, and the Moletronics Program of the Defense Advanced Research Projects Agency, the Microelectronics Advanced Research Corporation, its Focus Centers on Functional Engineered NanoArchitectonics and Advanced Materials and Devices, and the Center for Nanoscale Innovation for Defense.

Supporting information for this article is available on the WWW under <http://www.angewandte.org> or from the author.

tions. Most of these compounds have been studied<sup>[2,3,19]</sup> in the liquid-solution phase by using <sup>1</sup>H NMR spectroscopy and temperature-dependent electrochemistry. In addition, the switching cycle of a SAM<sup>[12]</sup> formed from a [2]rotaxane that is closely related to **R1<sup>4+</sup>** was previously reported. Herein, we present a description of the general switching cycle mechanism that is applicable to all four molecules, followed by a brief description of how certain details of this cycle vary between the four molecules.

The switching cycle mechanism for the bistable [2]catenanes and [2]rotaxanes is illustrated in Figure 2. There is always an equilibrium ( $K_{(D,T)^{4+}}$ ) established between the cyclobis(paraquat-*p*-phenylene) (CBPQT<sup>4+</sup>) ring encircling the tetrathiafulvalene (TTF) site (labeled as the ground-state co-conformer or GSCC) and the dioxynaphthalene (DNP) site (labeled as the metastable-state co-conformer or MSCC).<sup>[20]</sup> These labels reflect the fact that the equilibrium is most commonly shifted toward the CBPQT<sup>4+</sup> ring encircling the TTF site. The first oxidation state of the GSCC

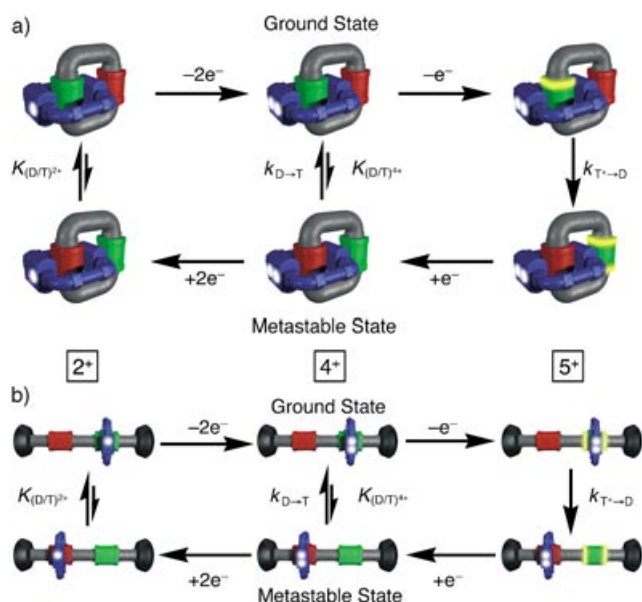


**Figure 2.** The analogous switching cycles for a) the bistable catenanes and b) the bistable rotaxanes, starting from the centrally located ground-state co-conformers. The green and red sites on the ring and dumbbell components refer to the TTF- and DNP-recognition units, respectively. When the TTF unit is oxidized, it is drawn as a highlighted green unit carrying yellow ends. The CBPQT<sup>4+</sup> ring is modeled as the blue ring encircling the green site with positive charges indicated as white spots. The metastable co-conformers are isomeric (and iso-electronic) with the appropriate ground-state co-conformers.

corresponds to removal of an electron from the TTF site, and is accompanied by a rapidly driven shuttling (Coulombic repulsion) of the CBPQT<sup>4+</sup> ring to the DNP site with a rate described by the constant,  $k_{T \rightarrow D}$ . Upon reduction of the TTF site back to its charge-neutral state, the MSCC is formed. The MSCC and GSCC are readily distinguished from each other by using CV because the oxidation potential of the (bare) TTF unit on the MSCC is approximately 200 mV less<sup>[12]</sup> positive than that for the GSCC (vs. a Pt reference electrode)—a result that is valid for both the bistable [2]catenanes and the bistable [2]rotaxanes. The return of the MSCC to the GSCC, which is really a recovery of the equilibrium distribution described by  $K_{(D/T)+}$ , is thermally activated. This recovery is typically too fast to observe at room temperature in the solution phase.

CV measurements on the bistable [2]rotaxane SAMs<sup>[12]</sup> revealed that the rate of recovery of the equilibrium distribution was strongly dependent<sup>[21]</sup> on the physical environment—the rate was much slower for the SAM environment than for the solution phase. For the SAM, it was also demonstrated that the GSCC/MSCC equilibrium distribution may be recovered at least 1000 times faster through the pathway that accesses the two-electron reduction of the CBPQT<sup>4+</sup> ring to its bis-radical cation, CBPQT<sup>2,2+</sup> (Figure 2).<sup>[12]</sup> This pathway is precisely that proposed originally as the mechanism for “opening” a MSTJ device.<sup>[13]</sup>

The solid-state polymer environment, which can be considered as a highly viscous solvent, should also affect the rate of recovery of the equilibrium distribution from the

MSCC to the GSCC. There is a long history, dating back to the early work of Kramers,<sup>[22]</sup> of investigations into molecular-mechanical processes within high-viscosity solvents,<sup>[23,24]</sup> although those studies have typically focused on low-amplitude molecular motions with energy barriers of only a few kcal mol<sup>-1</sup>. Based on the assumption that the large-amplitude, high-energy-barrier motions in our systems follow similar trends, the expectation is that the rate constant for the recovery of the equilibrium distribution will scale as  $k = \eta^{-\gamma}$  ( $\eta$  is the solvent viscosity and  $\gamma$  has a value between 0.5 and 0.75).<sup>[25]</sup>

The molecular switches investigated herein exhibit significant differences from one another that should be reflected in the switching characteristics of the electrochromic devices. **R1**<sup>4+</sup> and **R2**<sup>4+</sup> are characterized<sup>[3]</sup> by very different equilibrium dynamics in solution. **R1**<sup>4+</sup> contains a simple TTF unit, and the room-temperature affinity of the CBPQT<sup>4+</sup> ring for this TTF unit over the DNP ring system is 10:1. **R2**<sup>4+</sup> does not have a simple TTF unit and the CBPQT<sup>4+</sup> ring has an equal probability for being located on the “quasi-TTF” or the DNP at 298 K, although this equilibrium is temperature-dependent. As chemical constitution impacts the dynamic equilibrium between translational isomers<sup>[26]</sup> in solution for **R1**<sup>4+</sup> and **R2**<sup>4+</sup>, we expect a similar situation to pertain within the solid-state polymer environment.

**C1**<sup>4+</sup> and **C2**<sup>4+</sup>, on the other hand, are characterized<sup>[2,16]</sup> by similar equilibrium dynamics. For both structures, the ground-state equilibrium strongly favors the CBPQT<sup>4+</sup> ring encircling the TTF unit. However, the molecular-mechanical motion in **C2**<sup>4+</sup>, with its two bulky diazapyrenium units, is significantly more sterically hindered than that in **C1**<sup>4+</sup>, and this constitutional feature is expected, in any environment, to slow the recovery of **C2**<sup>4+</sup> from the MSCC to the GSCC substantially relative to that of **C1**<sup>4+</sup>.

Figure 3 shows two successive CVs collected from a solid-state polymer device containing **R1**<sup>4+</sup> as well as measurements

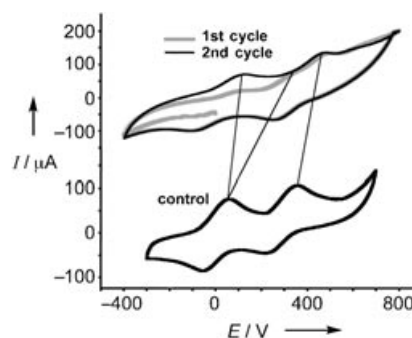


**Figure 3.** The first and second CVs (298 K, scan rate = 150 mVs<sup>-1</sup>) of the **R1**<sup>4+</sup>-containing solid-state polymer electrolyte device. The initial scan (gray trace) reveals a weak feature at 115 mV and two oxidation peaks (partially resolved) at 315 and 465 mV. For the second scan (black trace) virtually all the signal corresponding to the feature at 315 mV has shifted to 115 mV. The features at 115 and 315 mV were assigned as the first oxidation state of the metastable and ground-state co-conformers, respectively. A control device that contains only the dumbbell component of **R1**<sup>4+</sup> reveals two well-separated oxidation peaks at 55 and 355 mV that do not change between the first and second scans.

from a control device containing the dumbbell component of  $\mathbf{R1}^{4+}$ . This bistable [2]rotaxane exhibits an equilibrium GSCC/MSCC population of about 10:1 under ambient conditions, similar to that observed in solution at 298 K. The first CV trace reflects this distribution—three oxidation features are recorded at 115, 315, and 465 mV. The relatively weak feature at 115 mV corresponds to the  $\text{TTF} \rightarrow \text{TTF}^{+\cdot}$  oxidation of the low-abundance MSCC. The feature at 315 mV arises from the  $\text{TTF} \rightarrow \text{TTF}^{+\cdot}$  oxidation of the GSCC, and the feature at 465 mV is the second oxidation ( $\text{TTF}^{+\cdot} \rightarrow \text{TTF}^{2+}$ ) of  $\mathbf{R1}^{4+}$ . This second oxidation step is independent of the co-conformer as the CBPQT $^{4+}$  ring encircles the DNP site once the TTF site is singly oxidized. For the second scan, nearly all the integrated current under the 315 mV feature has moved to 115 mV. This assignment is consistent with the control device measurements, which reveal two well-separated oxidation peaks at 55 and 355 mV.

The hysteretic response in the successive CV curves of  $\mathbf{R1}^{4+}$  reflects the slow recovery of the ground-state equilibrium distribution (described by  $K_{(\text{D/T})^{++}}$ ), and is similar to that observed for the bistable [2]rotaxane SAMs.<sup>[12]</sup> By varying the time between the first and second CV scans as well as the temperature of the experiment, the various kinetic parameters for relaxation from the MSCC to the GSCC were determined. Figure 4a shows a scan-rate series of (second) CVs. Figure 4b displays a graph of the scan-rate series condensed into a single plot that exhibits an exponential decay. In this case, we have taken into account the rates based on the integrated current of the MSCC oxidation peak at 115 mV relative to the total current of the first-oxidation peaks of the MSCC and GSCC. For all data sets, at least one point was taken at scan rates that were much slower than the measured relaxation times—the  $\Delta t = 100$  s in Figure 4b, for example—and that point was fixed in the exponential decay fit. Figure 4c is an Eyring plot of several such series, each collected at a different temperature. From this plot, we can extract the various kinetic parameters that describe the recovery of the ground-state equilibrium distribution. Those parameters, along with the analogous measurements for  $\mathbf{C1}^{4+}$ ,  $\mathbf{C2}^{4+}$ , and  $\mathbf{R2}^{4+}$ , are summarized in Table 1. The data for  $\mathbf{C2}^{4+}$  were only collected under ambient conditions, and so only  $\tau_{298}$  and  $\Delta G_{298}^{\ddagger}$  are reported.

The polymer utilized in this case has a viscosity approximately  $10^4$  times greater than that of MeCN, which is the commonly used solvent in the investigation of the electrochemical properties of these molecules in solution. Thus, the implication is that the relaxation rates in solution should be between  $10^2$  and  $10^3$  times faster than those observed. Thus, under cryogenic conditions, it should be possible to observe the MSCC  $\rightarrow$  GSCC relaxation in the liquid-solution phase, and we have now confirmed that this prediction does, indeed, hold true.<sup>[19]</sup>

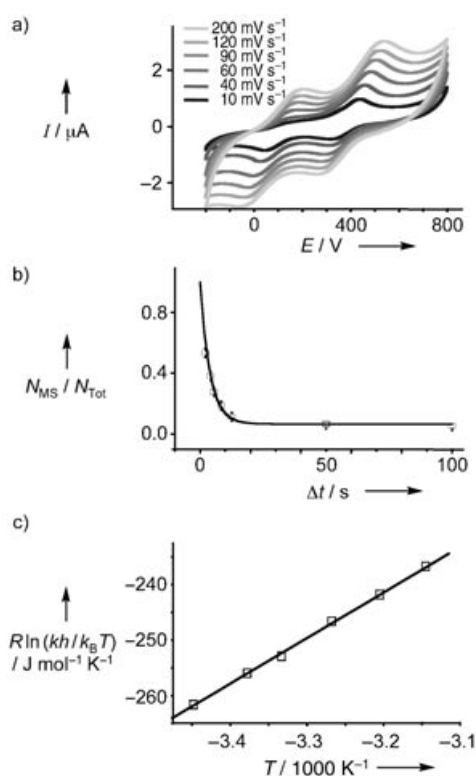


**Figure 4.** Experimental data utilized to extract the kinetic parameters of the metastable  $\rightarrow$  ground-state relaxation process of  $\mathbf{R1}^{4+}$  within the solid-state polymer electrolyte environment. a) Representative (second scan) CVs recorded at 296 K at various scan rates. b) The population ratios of the metastable state and the relaxation times fitted to a first-order decay model. c) The temperature dependence of the relaxation kinetics expressed as an Eyring plot.

**Table 1:** The  $1/e$  decay times ( $\tau_{298}$ ) and free energies of activation ( $\Delta G_{298}^{\ddagger}$ ) obtained by using cyclic voltammetry together with the thermodynamic data, obtained after an analysis of variable-temperature cyclic voltammetry studies using the Eyring ( $\Delta H^{\ddagger}$ ,  $\Delta S^{\ddagger}$ ) and the Arrhenius ( $E_a^{\ddagger}$ ) relationships for a series of bistable rotaxanes and catenanes in solution and in a solid-state polymer electrolyte.<sup>[a]</sup>

| Compound                              | $\tau_{298}$<br>[s] | $k_{298}$<br>[s $^{-1}$ ] | $\Delta G_{298}^{\ddagger}$<br>[kcal mol $^{-1}$ ] | $\Delta H^{\ddagger}$<br>[kcal mol $^{-1}$ ] | $\Delta S^{\ddagger}$<br>[cal mol $^{-1}$ K $^{-1}$ ] | $E_a^{\ddagger}$<br>[kcal mol $^{-1}$ ] |
|---------------------------------------|---------------------|---------------------------|--|--|---|---|
| [2] $\mathbf{R1}^{4+}$ <sup>[b]</sup> | 3.50 ( $\pm 0.02$ ) | 0.286 ( $\pm 0.002$ )     | 18.1 ( $\pm 0.2$ )                                 | 19.5 ( $\pm 0.2$ )                           | 4.7 ( $\pm 1.4$ )                                     | 19.6 ( $\pm 0.2$ )                      |
| [2] $\mathbf{R2}^{4+}$                | $\leq 1$            | $\geq 1$                  | 15.8 ( $\pm 0.4$ )                                 | 9.1 ( $\pm 0.4$ )                            | -22 ( $\pm 3$ )                                       | 9.7 ( $\pm 0.5$ )                       |
| [2] $\mathbf{C1}^{4+}$                | 0.6                 | 1.7                       | 17.0 ( $\pm 0.4$ )                                 | 14.8 ( $\pm 0.4$ )                           | -7.5 ( $\pm 2.5$ )                                    | 15.4 ( $\pm 0.4$ )                      |
| [2] $\mathbf{C2}^{4+}$                | 800                 | 0.00125                   | 21.0   | —  | —   | —                                       |

[a] Solid-state polymer data obtained from samples mixed within a polymer matrix (MeCN/PPMA/PC/LiClO $_4$  ( $w/w/w$ ) = 70:7:20:3) at a Pt electrode over a range of temperatures  $\mathbf{R1}^{4+}$  (290–320 K). [b] Self-assembled monolayers of the analogue to  $\mathbf{R1}^{4+}$ , bearing a disulfide tether, was characterized by variable-temperature CV to obtain thermodynamic data:  $k_{293} = 0.39$  s $^{-1}$ ,  $\Delta G_{298}^{\ddagger} = 18.0$  kcal mol $^{-1}$ ,  $\Delta H^{\ddagger} = 17.6 \pm 3.0$  kcal mol $^{-1}$ ,  $\Delta S^{\ddagger} = -1.4 \pm 10$  cal mol $^{-1}$  K $^{-1}$ ,  $E_a = 17.7 \pm 2.8$  kcal mol $^{-1}$ .

The viscosity of the polymer matrix changes by approximately a factor of two over the temperature range of these investigations (280–320 K). This trend can certainly impact the measured thermodynamic parameters—most notably  $\Delta S^{\ddagger}$ . However,  $\tau_{298}$ ,  $k_{298}$ ,  $\Delta G_{298}^{\ddagger}$ , and  $E_a$  are less sensitive and so it is in the case of these parameters that we have the most confidence. In reference to these values, we find that the MSCC  $\rightarrow$  GSCC relaxation rates, within the polymer environment, are under significant chemical control. In fact, they

varied by more than 1000 times in moving from  $R2^{4+}$  to  $C2^{4+}$ . This result directly translates into chemical control over colorimetric retention times in these electrochromic devices. In Figure 5, we present a demonstration of such a device

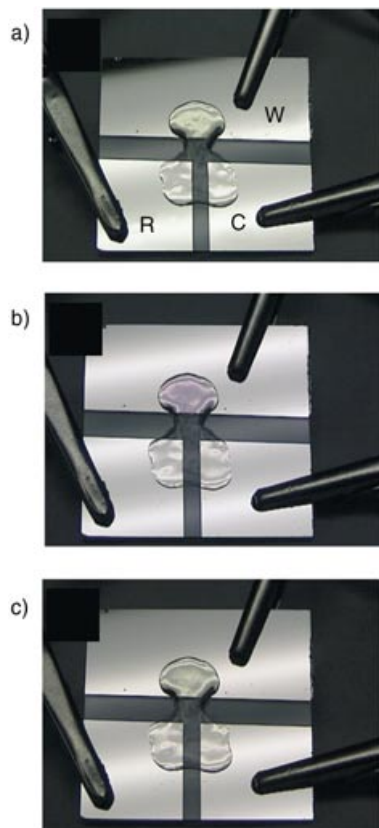


**Figure 5.** The electrochromic response of the solid-state polymer devices. The working (W), counter (C), and reference (R) electrodes are indicated. a) The device with the working electrode grounded. The green color correlates with the color of the ground-state co-conformer of  $R1^{4+}$ , with the CBPQT $^{4+}$  ring encircling the TTF site. b) After a +1 V oxidizing potential has been applied to the working electrode, the color change to red/purple correlates with the translational isomerization having occurred to the metastable state. c) Several seconds after the working electrode has been returned to 0 bias and  $R1^{4+}$  has relaxed back to the ground-state co-conformer.

containing  $R1^{4+}$  that was cycled from the green to the red state, and then back to the green state again. This electrochromic device<sup>[27]</sup> contained substantially higher concentrations of  $R1^{4+}$  than did other devices discussed herein, but was, in all other ways, identical to them.

In summary, we find that a single mechanistic picture can be applied to describe the electrochemically driven switching cycle of bistable [2]catenanes and [2]rotaxanes in solid-state polymer electrolytes. This mechanistic picture is qualitatively identical to that initially proposed to describe the behavior of a MSTJ device,<sup>[13]</sup> and is also analogous to that observed for the switching cycle of a [2]rotaxane SAM.<sup>[12]</sup> We find that the MSCC→GSCC relaxation rate is strongly dependent upon both physical environment and molecular structure. In particular, by varying the molecular structure we could vary

this relaxation rate by more than 1000 times. This variation has interesting implications for controlling the colorimetric retention times (and hence power efficiencies) in solid-state electrochromic devices,<sup>[27]</sup> and we have demonstrated such a device. Finally, these results suggest that electrochemical measurements<sup>[19]</sup> on these same molecules in cryogenic solutions should go far toward quantifying how the kinetic parameters that describe the switching cycle are impacted by the physical environment of the molecular switches.

### Experimental Section

A three-terminal, microfabricated device, operated as a function of voltage scan rate and temperature, was employed to interrogate the kinetics of electrochemically-induced molecular mechanical switching within a solid-state polymer. The polymer electrolyte matrix was a standard solid-state electrolyte prepared from a solution in MeCN that contained polymethylmethacrylate (PMMA,  $M_w = 300\,000$ ), propylene carbonate, (PC)—as a plasticizer—and  $LiClO_4$  (MeCN/PMMA/PC/ $LiClO_4$  (w/w/w/w) = 70:7:20:3). These materials were handled only in flame-dried glassware under an inert atmosphere of Ar. The  $LiClO_4$  was purified by fusion under vacuum. The MeCN was dried either by passage through steel columns containing activated alumina under Ar using a solvent purification system (Anhydrous Engineering) or by distillation over  $CaH_2$ . Finally, the MeCN was deoxygenated prior to use through three freeze/pump/thaw cycles.

The solid-state electrolyte devices were fabricated with traditional CV experiments in mind. A planar three-electrode—working, counter, reference—configuration was implemented, and each electrode consisted of 10 nm of Ti covered with 50 nm of Pt. The electrodes were patterned by using standard lithographic and metal evaporation procedures onto a glass substrate. The fabricated substrates were placed in a glove box under a  $N_2$  environment. The electrochemically active species were then combined with the electrolyte and drop cast onto the three electrodes. These devices were allowed to stand for 20 min to facilitate drying, and then were pumped for a further 20 min to a final pressure of 100 mTorr. The working devices were firm to the touch, with a consistency similar to that of a stiff rubber band. The viscosity of similarly prepared polymer electrolytes has been reported,<sup>[28]</sup> and, at 298 K, it is more than  $10^4$  times larger than that for the solvent MeCN.

CV measurements were performed in a sealed container on an EG&G VersaStat II Potentiostat with the aid of three electrical feedthroughs and a thermocouple fed back to a hot-plate for thermal control. The key experimental variables were scan rate and temperature and—for a given device—these parameters were varied randomly to avoid the influence of systematic errors.

Received: August 19, 2004

**Keywords:** catenanes · electrochromic devices · metastable compounds · polymers · rotaxanes

- [1] R. A. Bissell, E. Córdova, A. E. Kaifer, J. F. Stoddart, *Nature* **1994**, *369*, 133–137.
- [2] a) M. Asakawa, P. R. Ashton, V. Balzani, A. Credi, C. Hamers, G. Mattersteig, M. Montalti, A. N. Shipway, N. Spencer, J. F. Stoddart, M. S. Tolley, M. Venturi, A. J. P. White, D. J. Williams, *Angew. Chem.* **1998**, *110*, 357–361; *Angew. Chem. Int. Ed.* **1998**, *37*, 333–337; b) V. Balzani, A. Credi, G. Mattersteig, O. A. Matthews, F. M. Raymo, J. F. Stoddart, M. Venturi, A. J. P. White, D. J. Williams, *J. Org. Chem.* **2000**, *65*, 1924–1936.
- [3] a) J. O. Jeppesen, K. A. Nielsen, J. Perkins, S. A. Vignon, A. Di Fabio, R. Ballardini, M. T. Gandolfi, M. Venturi, V. Balzani, J.

- Becher, J. F. Stoddart, *Chem. Eur. J.* **2003**, *9*, 2982–3007; b) T. Yamamoto, H.-R. Tseng, J. F. Stoddart, V. Balzani, A. Credi, F. Marchioni, M. Venturi, *Collect. Czech. Chem. Commun.* **2003**, *68*, 1488–1514; c) H.-R. Tseng, S. A. Vignon, P. C. Celestre, J. Perkins, J. O. Jeppesen, A. Di Fabio, R. Ballardini, M. T. Gandolfi, M. Venturi, V. Balzani, J. F. Stoddart, *Chem. Eur. J.* **2004**, *10*, 155–172.
- [4] V. Balzani, A. Credi, M. Venturi, *Molecular Devices and Machines—A Journey into the Nano World*, Wiley-VCH, Weinheim, **2003**.
- [5] a) J. F. Stoddart, *Chem. Aust.* **1992**, *59*, 576–577, 581; b) A. N. Shipway, I. Willner, *Acc. Chem. Res.* **2001**, *34*, 421–432; c) B. X. Colasson, C. Dietrich-Buchecker, M. C. Jimenez-Molero, J.-P. Sauvage, *J. Phys. Org. Chem.* **2002**, *15*, 476–483; d) M. Cavallini, F. Biscarini, S. Leon, F. Zerbetto, G. Bottari, D. A. Leigh, *Science* **2003**, *299*, 531–531; e) A. H. Flood, R. J. A. Ramirez, W.-Q. Deng, R. P. Muller, W. A. Goddard III, J. F. Stoddart, *Aust. J. Chem.* **2004**, *57*, 301–322; f) P. H. Kwan, M. J. MacLachlan, T. M. Swager, *J. Am. Chem. Soc.* **2004**, *126*, 8638–8639.
- [6] a) For an example of working supramolecular machines in the form of [2]pseudorotaxanes trapped in glass and mounted on the surface of a silica film, see: S. Chia, J. Cao, J. F. Stoddart, J. I. Zink, *Angew. Chem.* **2001**, *113*, 2513–2517; *Angew. Chem. Int. Ed.* **2001**, *40*, 2447–2451; b) for a recent example in which a [2]pseudorotaxane, as a self-assembled monolayer on gold, was shown to undergo reversible dethreading and rethreading of its ring, and so exhibit ion-gating behavior; see: K. Kim, W. S. Jeon, J.-K. Kang, J. W. Lee, S. Y. Jon, T. Kim, K. Kim, *Angew. Chem.* **2003**, *115*, 2395–2398; *Angew. Chem. Int. Ed.* **2003**, *42*, 2293–2296; c) for a detailed discussion on the assembly of an electronically switchable rotaxane on the surface of a titanium dioxide nanoparticle, see: B. Long, K. Nikitin, D. Fitzmaurice, *J. Am. Chem. Soc.* **2003**, *125*, 15490–15498; d) for a very recent example of a functioning nanomachine in the form of a supramolecular nanovalve that opens and closes the orifices to molecular-sized pores and releases a small number of molecules on demand, see: R. Hernandez, H.-R. Tseng, J. W. Wong, J. F. Stoddart, J. I. Zink, *J. Am. Chem. Soc.* **2004**, *126*, 3370–3371; e) in a very recent study, a novel method was demonstrated for the electrical contacting of a redox enzyme by using the CBPQT<sup>4+</sup> ring as a rotaxane-derived electronic relay on a molecular wire connecting the enzyme to the electrode; see: E. Katz, L. Sheeney-Haj-Idchia, I. Willner, *Angew. Chem.* **2004**, *116*, 3354–3362; *Angew. Chem. Int. Ed.* **2004**, *43*, 3292–3300.
- [7] For a very early example of self-assembling a donor–acceptor [2]catenane-like structure on a gold surface, see: T. Lu, L. Zhang, G. W. Gokel, A. E. Kaifer, *J. Am. Chem. Soc.* **1993**, *115*, 2542–2543.
- [8] For a discussion of the current/voltage characteristics of Langmuir–Blodgett monolayers of redox-switchable [2]catenanes on gold, see: M. Asakawa, M. Higuchi, G. Mattersteig, T. Nakamura, A. R. Pease, F. M. Raymo, T. Shimizu, J. F. Stoddart, *Adv. Mater.* **2000**, *12*, 1099–1107.
- [9] Recently, it was demonstrated that an array of microcantilever beams, when coated with a SAM of palindromic, bistable [3]rotaxane molecules, undergoes controllable and reversible bending when it is exposed to chemical oxidants and reductants; see: T. J. Huang, B. Brough, C.-M. Ho, Y. Liu, A. H. Flood, P. A. Bonvallet, H.-R. Tseng, J. F. Stoddart, M. Baller, S. Magonov, *Appl. Phys. Lett.* **2004**, *85*, in press.
- [10] I. C. Lee, C. W. Frank, T. Yamamoto, H.-R. Tseng, A. H. Flood, J. F. Stoddart, J. O. Jeppesen, *Langmuir* **2004**, *20*, 5809–5828.
- [11] For evidence that redox-controllable molecular shuttles, in the form of amphiphilic, bistable [2]rotaxanes, are mechanically switchable with chemical reagents in closely packed Langmuir films, and in Langmuir–Blodgett bilayers mounted on solid substrates, see: T. J. Huang, H.-R. Tseng, J. Sha, W. Lu, B. Brough, A. H. Flood, B.-D. Yu, P. C. Celestre, J. P. Chang, J. F. Stoddart, C.-M. Ho, *Nano Lett.* **2004**, *4*, ASAP.
- [12] H.-R. Tseng, D. Wu, N. X. Fang, X. Zhang, J. F. Stoddart, *ChemPhysChem* **2004**, *5*, 111–116.
- [13] C. P. Collier, G. Mathersteig, E. W. Wong, Y. Luo, K. Beverly, J. Sampaio, F. M. Raymo, J. F. Stoddart, J. R. Heath, *Science* **2000**, *289*, 1172–1175.
- [14] C. P. Collier, J. O. Jeppesen, Y. Luo, J. Perkins, E. W. Wong, J. R. Heath, J. F. Stoddart, *J. Am. Chem. Soc.* **2001**, *123*, 12632–12641.
- [15] Y. Luo, C. P. Collier, J. O. Jeppesen, K. A. Nielsen, E. De Ionno, G. Ho, J. Perkins, H.-R. Tseng, T. Yamamoto, J. F. Stoddart, J. R. Heath, *ChemPhysChem* **2002**, *3*, 519–525.
- [16] M. R. Diehl, D. W. Steuerman, H.-R. Tseng, S. A. Vignon, A. Star, P. C. Celestre, J. F. Stoddart, J. R. Heath, *ChemPhysChem* **2003**, *4*, 1335–1339.
- [17] P. R. Ashton, S. E. Boyd, A. Brindle, S. J. Langford, S. Menzer, L. Pérez-García, J. A. Preece, F. M. Raymo, N. Spencer, J. F. Stoddart, A. J. P. White, D. J. Williams, *New J. Chem.* **1999**, *23*, 587–602.
- [18] The synthesis of rotaxane **R1**<sup>4+</sup> and its corresponding dumbbell are reported in the Supporting Information.
- [19] A. H. Flood, A. J. Peters, S. A. Vignon, D. W. Steuerman, H.-R. Tseng, J. R. Heath, J. F. Stoddart, *Chem. Eur. J.* **2004**, *10*, 6558–6561.
- [20] Previously, we had advocated (M. C. T. Fyfe, P. T. Glink, S. Menzer, J. F. Stoddart, A. J. P. White, D. J. Williams, *Angew. Chem.* **1997**, *109*, 2158–2160; *Angew. Chem. Int. Ed. Engl.* **1997**, *36*, 2068–2070) the use of the term “co-conformation” to designate the different three-dimensional spatial arrangements of the components of mechanically interlocked molecular systems. Also, in identifying the ON and OFF states of the bistable [2]catenane employed in the first MSTJ crossbar device,<sup>[16]</sup> we employed the term “co-conformer” to the two states. See, especially Figure 1 in reference [16]. In other words, in proposing our original mechanism, we appreciated correctly that the ON and OFF states are both isomeric and, of course, isoelectronic.
- [21] SAMs of copper catenates have been prepared; however, the electrochemically-triggered circumrotations are either significantly slower than the corresponding motions in solution or completely frozen out; see: L. Raehm, J.-M. Kern, J.-P. Sauvage, C. Hamann, S. Palacin, J.-P. Bourgoin, *Chem. Eur. J.* **2002**, *8*, 2153–2162.
- [22] H. A. Kramers, *Physica* **1940**, *7*, 284–304.
- [23] D. Raftery, R. J. Senson, R. M. Hochstrasser in *Activated Barrier Crossings* (Eds: G. Fleming, R. Hanggi), World Scientific, Hackensack, NJ, **1993**, p. 163.
- [24] a) R. F. Grote, J. T. Hynes, *J. Chem. Phys.* **1980**, *73*, 2715–2732; b) R. F. Grote, J. T. Hynes, *J. Chem. Phys.* **1981**, *74*, 4465–4475.
- [25] a) H. Sumi, R. A. Marcus, *J. Chem. Phys.* **1986**, *84*, 4894–4914; b) H. Sumi, *J. Mol. Liq.* **1993**, *65*, 65–73.
- [26] G. Schill, K. Rissler, W. Vetter, *Angew. Chem.* **1981**, *93*, 197–201; *Angew. Chem. Int. Ed. Engl.* **1981**, *20*, 187–189.
- [27] a) For a general discussion of electrochromic devices, see: D. R. Rossinsky, R. J. Mortimer, *Adv. Mater.* **2001**, *13*, 783–793; b) see also the Special Issue covering the Third International Meeting on Electrochromics (IME-3) in *Electrochimica Acta* **1999**, *44*(18), 2969–3258; c) Electrochromic devices have been developed out of a variety of different materials; for examples of molecular systems, see: R. J. Mortimer, *Electrochim. Acta* **1999**, *44*, 2971–2981, and, for an example in which an electrochromic molecule that has been attached to a solid support, see: R. Cinnsealach, G. Boschloo, S. Nagaraja Rao, D. Fitzmaurice, *Sol. Energy Mater. Sol. Cells* **1999**, *57*, 107–125; for examples of polymers, see: F. Fungo, S. A. Jenekhe, A. J. Bard, *Chem. Mater.* **2003**, *15*, 1264–1272, and, for a very recent report on polymeric

- systems, see: G. Sonmez, C. K. F. Shen, Y. Rubin, F. Wudl, *Angew. Chem.* **2004**, *116*, 1524–1528; *Angew. Chem. Int. Ed.* **2004**, *43*, 1498–1502; for examples of metal-oxide thin films, see: S. Papaefthimiou, G. Leftheriotis, P. Yianoulis, *Electrochim. Acta* **2001**, *46*, 2145–2150; d) for the use of polymer-gel electrolytes in electrochromic devices, see: J. Vondrák, M. Sedlarikova, J. Reiter, T. Hodal, *Electrochim. Acta* **1999**, *44*, 3067–3073.
- [28] M. Deepa, N. Sharma, S. A. Agnihory, S. Singh, T. Lal, R. Chandra, *Solid State Ionics* **2002**, *152–153*, 253–258.